Formation of garnet-type $Li_7La_3Zr_2O_{12}$ nanoparticles as an alternative structural stabilization route

RS Ledwaba,* PE Ngoepe

Materials Modelling Centre, University of Limpopo, Private Bag x1106, Sovenga, 0727, South Africa
Email: raesibe.ledwaba@ul.ac.za

Abstract

The cubic garnet-type $Li_7La_3Zr_2O_{12}$ (LLZO) is an eminent candidate for next-generation solid state battery technology due to its thermal stability and high ionic conductivity. As such, its operation mechanisms need to be thoroughly understood, particularly on the structural instability challenge reported to occur at lower temperatures. Although it exists as either the tetragonal or cubic structures, the latter is favourable because of its higher Li^+ conductivity rate. However, inability to retain thermodynamic stability in cubic phase at low temperatures ($\leq$ 903,15 K) remains a challenge. As an alternative to extrinsic doping, as recently attempted in various studies, it has been discovered that decreasing the size to nano-level could remedy the phase stability challenge of cubic LLZO. Herein, we have modelled the bulk and nanostructured LLZO under various temperature conditions in the range 300 – 1500 K using the DL_ POLY molecular dynamics code, to understand the LLZO high temperature behaviour and track phase transformations. The molecular dynamics calculations performed on these materials revealed two distinct patterns of Li-ion transport on the diffusion coefficient plots. The trends in conductive ion diffusions show that nanostructured materials yield higher diffusion coefficients that the bulk structures. Findings of this study form a strong foundation towards the amorphization and recrystallization of these materials to monitor any change in structure post crystallization since the ability to retain both structural and conductivity rate are equally crucial.

1. Introduction

Significant interest has been devoted towards the development of lithium ion conductive solid electrolytes *in a quest to substitute the flammable, volatile and unstable organic liquid-based electrolytes amid their safety* (Karabelli et al. 2021). The solid state battery technology reigns as a promising alternative, with fast lithium-ion diffusion, and immense potential to addressing thermal and chemical stability shortfalls of liquid-electrolytes. Utilisation of solid electrolytes opens a wider operational temperature window and promises improved architectural design for all-solid-state batteries (ASSBs) to be utilised in the next-generation energy storage technology with excellent chemical and electrochemical stability (Xu et al. 2012). Inorganic oxide lithium ion conductors *have been reported to be superior to non-oxides for their good handling, chemical and electrochemical stability, particularly, the zirconium-containing lithium–lanthanum–oxide ($Li_7La_3Zr_2O_{12}$ / LLZO). The $Li_7La_3Zr_2O_{12}$* has increased safety coupled with enhanced Li-ion conductivity. However, its highly conductive cubic phase is unstable at room temperature and undergoes transformation to a low ionic conductive tetragonal phase (Li and Wang. 2021).

Exploration of size variation to stabilize the cubic phase in LLZO may be a viable alternative to extrinsic doping as recently discovered. This was evident when nanostructured LLZO, was observed to remain stable as c-LLZO at room temperature without the use of dopants (Gordon et al. 2015). In their unique nature, nanomaterials have surface effect that are far greater than those of bulk and microscale solids, which is ascribed to their huge specific surface area. Hence their distinctly different properties compared with those of macroscopic materials. Consequently, it is crucial
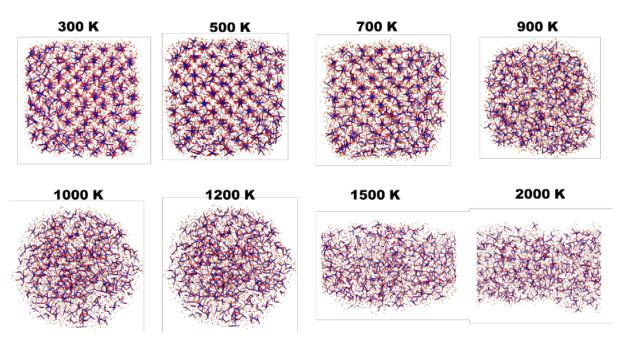
to investigate the evolution process of nanostructured LLZO in a quest to study the structural and dynamic properties that influence the electrochemical performance of electrolyte materials. However, the structural complexity in this garnet-type crystal hampers the understanding of the mechanism of Li-ion transport and also adds difficulty to the improvement of such electrolytes (Xu et al. 2012).

Numerous theoretical studies used to investigate the structure and energetics of a system proceed by proposing an atomistic model, which was then simulated using static or dynamical methods. Molecular dynamics (MD) simulation is an effective approach to simulate the atomic motion based on the Newtonian mechanics, which has been widely adopted by numerous scholars to examine the melting mechanism and thermally-stimulated migration of lithium ions mainly because in most instances, they cannot be accurately observed and measured through the conventional experimental approaches. As such, it is of great importance to develop a suitable method to prepare nano LLZO precursor powders with high purity as well as homogeneity (Zhang et al. 2015).

Herein the high temperature behaviour of LLZO is carefully investigated as an initial step to identifying the high temperature behaviour of this electrolyte material. Subsequently, employment of the armorphization and recrystallization process (Ledwaba et al. 2020; Shibiri et al. 2019) will be of essence as this process helps with the unique acquisition of the microstructural properties and eventually the prediction of performance-enhancing properties for the ultimate improvement of all solid state batteries.

2. Computational Procedure

The classical molecular dynamics simulations of LLZO have been performed using the DLPOLY classical code (Smith and

Figure 1: Snapshots of the atom positions comprising the $Li_7La_3Zr_2O_{12}$ nanoparticle, taken as a function of temperature, illustrating the amorphization process. Species colored blue correspond to zirconium and are bonded oxygen atoms in red to illustrate more clearly the Zr-O octahedral co-ordination and connectivity. The figures were constructed to ensure clarity of the amorphization and formation of the various nanostructural morphologies due to temperature

Forester 1996), and the Born Model of ionic solids was utilized for describing atom interactions within the systems. The buckingham interatomic potential derived by Wang (Wang et al. 2014). The bulk and nanoparticles (8nm) of $Li_7La_3Zr_2O_{12}$ were generated using the METADISE code (Watson et al. 1996). The models containing 5184 atoms, were generated together with input files for the DL_ POLY code corresponding to the structural parameters. The high temperature simulations were performed using the micro-canonical ensemble (NVE -constant number of atoms, constant volume, and constant energy) at different temperatures in the range 300 K to 1500 K.
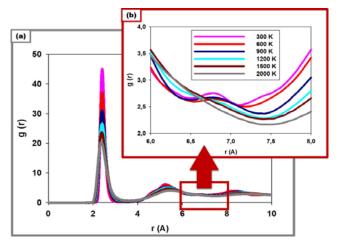
3.   Results and Discussions

3.1   Structural Dynamics

Molecular graphics visualization is central to this study for systematic monitoring of temperature effects and capturing the desired amorphization temperature for the solid electrolyte material. In figure 1, the line representation of LLZO is shown with the blue representing zirconium and red representing oxygens. The snapshots of the LLZO nanoparticles are illustrated to help describe the amorphization process due taking place due to temperature variation. The snapshots at 300 and 500 K illustrate ordered structures implying that the nanoparticle is still in crystalline form. Partial disordering occurs at the edges of the structure when heated up to 700 K. After 900 K, the edges of the LLZO structure smoothen into a spherical shape and the atomic arrangement appears to be disordered. At 1000 K and 1200 K, the desired nanosphere emerges and beyond the 1200 K temperature, then shape of LLZO now transitions into a rod-like type of structure. This is in line with the experimental observation that the LLZO nanostructure reaches its sintering temperature at $1230°C$ (~1503 K) (Murugan et al. 2007) i.e the system temperature at which the particles contact and connect with each other.

3.2   Radial Distribution Functions

In this section, the radial distribution functions (RDF) are employed to help determine the melting temperature of the nanostructured LLZO material. This is due to the essence of melting mechanism in relation to the amorphization process of materials and renders RDFs instrumental to show when the entire system begins to melt. RDF graphs are an essential tool to depict the occurrence probability of other particles around the coordinates of a specific particle within a certain range (cutoff radius), hence their capability to describe orderliness of the particle. Figure 2, illustrates the RDF graphs for the Zr-O interaction during temperature various, suggesting that only the interactions between particles within the 10 Å range were taken into consideration. At lower temperature 300 and 600K, represented by the pink and red colours, respectively; the RDF displayed relatively ordered peaks, demonstrating that all particles in the entire system were orderly arranged at this moment. The rdf peaks are well defined and represent an ordered system. This is in agreement with the snapshots of the images in figure 1. However, at T = 900 K, these peaks were notably reduced as the temperature elevated. Specifically, the 6 curves in different colors from the top to the bottom represented the RDF curves at the temperature of T = 300 K to T = 2000 K, and the value of the third peak was reduced as the temperature increased. In addition, the flat degree of curve (disordering) was also enhanced with the increase in temperature. Noteworthily, the third peak was decreased again and then tended to be gentle, while the entire RDF values showed that the overall trend of atoms was ordering at the short range whereas disordering within the long range, revealing that the particles under such temperature entered the disordering status (melting status) Accordingly, the magnification of around 6-8 Å (red box), clearly displayed its variation trend; as a result, the melting temperature Tm was determined. Beyond T = 1200 K the same flat degree occurred near the third peaks of the three curves, indicating that

Figure 2: Radial distribution function graphs for Zr-O interactions at within the LLZO nanostructure at temperature ranges 300 -1500 K within a (a)10 Å cutoff radius and (b) magnification of the 6 to 8 Å region.

the system showed the disordered state within such a temperature range (the melting state). To sum up, the melting temperature of the present LLZO should be set within the range of T = 900 K to T = 1200 K.

3.3 Dynamic Properties

The lithium ion diffusion coefficients are illustrated in figure 3 for the bulk and nanostructed LLZO solid electrolyte materials. In (a), the diffusion rate around room temperature occurs at a rate of 2,82E-03 nm²/s followed by a slight declined to 1,65E-03 nm²/s at 500 K. This is followed by a gradual increase with an increase in temperature all the way to 1,78E-01 nm²/s at 1500 K. In the case of nanostructured LLZO (b), the lithium ion diffusion coefficients starts as 1,84 nm²/s at room temperature then decreases to 3,06E-

01 nm²/s and 2,92E-01 nm²/s at 500 and 600 K, respectively. It then inclines sharply to 2,76 nm²/s at 700 K and hits a lower point at 800 K. This is folloewd by a steady increase in diffusivity all the way to 4,84 nm²/s at 1500 K. It is evident that in both graphs, the materials undergoes a transition around 500 K (Zhang et al. 2014) that ignited interest apart from the tetragonal to cubic transition previously. Figure 3(c) display a variation in diffusion by a magnitude of 3 at room temperature and a magnitude of 2 for the nanostructured morphologies at 1000 and 1200 K. Preliminary as is, these results show without doubt that nanostructured LLZO has higher conductive ion diffusion than its counterpart.

Conclusion

In the current work, molecular dynamics simulations were instrumental in providing insights on the structural behavior of bulk and nanosized LLZO electrolyte material. Our results show that the structural ordering in the material coincides with that is predicted in literature regarding the difference in properties when migrating to nanoscale. This sets a strong foundation for future amorphisation and recrystallization work of nanostructures aimed to improve the ionic conductivity of the LLZO electrolyte.

ORCID

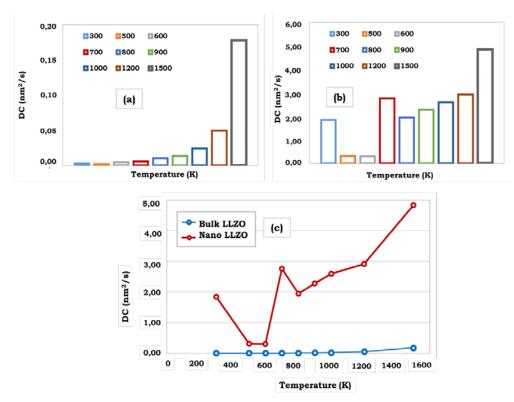Raesibe S. Ledwaba

https://orcid.org/0000-0001-5807-5177

Figure 3: Diffusion Coefficients of LLZO (a) bulk, (b) nanostructure and (c) superimposed bulk and nanostructured.

Phuti E. Ngoepe

https://orcid.org/0000-0003-0523-5602

References

1. Gordon Z.D., Yang T., Gomes Morgado G. B. and Chan C. K. 2016, Preparation of Nano- and Microstructured Garnet $Li_7La_3Zr_2O_{12}$ Solid Electrolytes for Li-Ion Batteries via Cellulose Templating ACS Sustainable Chemistry & Engineering 4, 6391-6398

2. Karabelli D., Birke K. P. and Weeber M., 2021. A Performance and Cost Overview of Selected Solid-State Electrolytes: Race between Polymer Electrolytes and Inorganic Sulfide Electrolytes. Batteries 7, 18

3. Kumar P. J., Nishimura K., Senna M., Düvel A., Heitjans, P., Kawaguchi T., Sakamoto N., Wakiya N. and Suzuki H., 2016. A novel low-temperature solid-state route for nanostructured cubic garnet $Li_7La_3Zr_2O_{12}$ and its application to Li-ion battery RSC Advances 6, 62656-62667

4. Ledwaba R S, Sayle D C and Ngoepe P E 2020 ACS Applied Energy Materials 3 1429-1438

5. Li J. and Wang R., 2021. Recent advances in the interfacial stability, design and in situ characterization of garnet-type $Li_7La_3Zr_2O_{12}$ solid-state electrolytes based lithium metal batteries. Ceramics International 47, 13280-13290

6. Murugan R., Thangadurai V. and Weppner W 2007. Fast Lithium Ion Conduction in Garnet-Type $Li_7La_3Zr_2O_{12}$. Angewandte Chemie International Edition 46, 7778-7781

7. Shibiri B., Ledwaba R. S. and Ngoepe P. E., 2019. Discharge induced structural variation of simulated bulk $Li_{1+x}Mn_2O_4$ ($0\leq$ x$\leq$ 1). Optical Materials 92, 67-70

8. Smith W and Forester T R DL_POLY_2. 0: A general-purpose parallel molecular dynamics simulation package1996 Journal of Molecular Graphics 14 136-141

9. Wang Y., Huq A. and Lai W., 2014. Insight into lithium distribution in lithium-stuffed garnet oxides through neutron diffraction and atomistic simulation: $Li_{7-x}La_3Zr_{2-x}Ta_xO_{12}$ (x= 0–2) series. Solid State Ionics 255, 39-49

10. Watson G. W., Kelsey E. T., De Leeuw N. H., Harris D. J. and Parker S. C., 1996. Atomistic simulation of dislocations, surfaces and interfaces in MgO. Journal of the Chemical Society 92, 433-438

11. Xu M., Park M. S., Lee J.M., Kim T.Y., Park Y.S. and Ma E., 2012. Mechanisms of Li$^+$ transport in garnet-type cubic $Li_{3+x}La_3M_2O_{12}$ (M= Te, Nb, Zr). Physical Review B 85, 052301

12. Yang .T, Gordon Z. D., Li Y. and Chan C. K., 2015. Nanostructured garnet-type solid electrolytes for lithium batteries: electrospinning synthesis of $Li_7La_3Zr_2O_{12}$ nanowires and particle size-dependent phase transformation. The Journal of Physical Chemistry C 119 14947-14953

13. Zhang Y., Cai J., Chen F., Tu R., Shen Q., Zhang X. and Zhang L., 2015. Preparation of cubic $Li_7La_3Zr_2O_{12}$ solid electrolyte using a nano-sized core–shell structured precursor. Journal of Alloys and Compounds 644, 793-798

14. Zhang Y., Chen F., Tu R., Shen Q. and Zhang L., 2014. Field assisted sintering of dense Al-substituted cubic phase $Li_7La_3Zr_2O_{12}$ solid electrolytes. Journal of Power Sources 268, 960-964